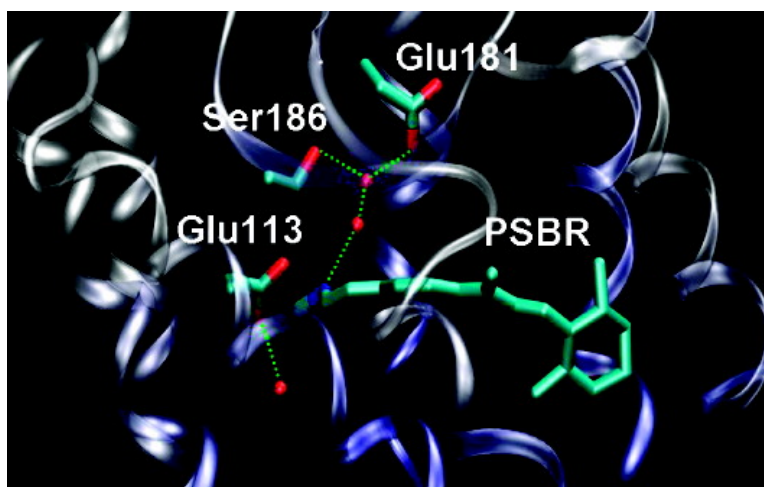


An Opsin Shift in Rhodopsin: Retinal S0–S1 Excitation in Protein, in Solution, and in the Gas Phase

Ksenia Bravaya, Anastasia Bochenkova, Alexander Granovsky, and Alexander Nemukhin

J. Am. Chem. Soc., **2007**, 129 (43), 13035-13042 • DOI: 10.1021/ja0732126 • Publication Date (Web): 09 October 2007

Downloaded from <http://pubs.acs.org> on February 14, 2009



More About This Article

Additional resources and features associated with this article are available within the HTML version:

- Supporting Information
- Links to the 6 articles that cite this article, as of the time of this article download
- Access to high resolution figures
- Links to articles and content related to this article
- Copyright permission to reproduce figures and/or text from this article

[View the Full Text HTML](#)

An Opsin Shift in Rhodopsin: Retinal S0–S1 Excitation in Protein, in Solution, and in the Gas Phase

Ksenia Bravaya,[‡] Anastasia Bochenkova,^{*‡} Alexander Granovsky,[‡] and Alexander Nemukhin^{†‡}

Contribution from the Department of Chemistry, M.V. Lomonosov Moscow State University, 1/3, Leninskie Gory, Moscow, 119992, Russian Federation, and N. M. Emanuel Institute of Biochemical Physics, Russian Academy of Sciences, 4, ul. Kosygina, Moscow, 119994, Russian Federation

Received May 7, 2007; E-mail: anastasia.bochenkova@gmail.com

Abstract: We considered a series of model systems for treating the photoabsorption of the 11-*cis* retinal chromophore in the protonated Schiff-base form in vacuum, solutions, and the protein environment. A high computational level, including the quantum mechanical–molecular mechanical (QM/MM) approach for solution and protein was utilized in simulations. The S0–S1 excitation energies in quantum subsystems were evaluated by means of an augmented version of the multiconfigurational quasidegenerate perturbation theory (aug-MCQDPT2) with the ground-state geometry parameters optimized in the density functional theory PBE0/cc-pVDZ approximation. The computed positions of absorption bands λ_{\max} , 599(g), 448(s), and 515(p) nm for the gas phase, solution, and protein, respectively, are in excellent agreement with the corresponding experimental data, 610(g), 445(s), and 500(p) nm. Such consistency provides a support for the formulated qualitative conclusions on the role of the chromophore geometry, environmental electrostatic field, and the counterion in different media. An essentially nonplanar geometry conformation of the chromophore group in the region of the C14–C15 bond was obtained for the protein, in particular, owing to the presence of the neighboring charged amino acid residue Glu181. Nonplanarity of the C14–C15 bond region along with the influence of the negatively charged counterions Glu181 and Glu113 are found to be important to reproduce the spectroscopic features of retinal chromophore inside the Rh cavity. Furthermore, the protein field is responsible for the largest bond-order decrease at the C11–C12 double bond upon excitation, which may be the reason for the 11-*cis* photoisomerization specificity.

Introduction

Retinal proteins play a crucial role in different biophysical processes including visual signal transduction by rhodopsin (Rh)^{1–3} and other visual pigments, ion transport through the cell membrane, and photoreception. Utilizing the retinal molecule as a chromophore group these proteins absorb light in the wide range of UV/visible spectra with absorption maxima located between 360 and 635 nm. The spectral tuning is caused by diverse influence of the protein environment on the chromophore group. According to the results of crystallographic studies^{4–7} rhodopsin comprises seven-helical transmembrane apoprotein opsin with a covalently bound chromophore group of 11-*cis* retinal. The covalent linkage is obtained by the

formation of a protonated Schiff base of retinal (PSBR) by the amino end of the Lys296 residue and the carbonyl moiety of retinal. PSBR positive charge is stabilized by the carboxyl group of Glu113^{8,9} (Scheme 1). The primary event of the visual signal transduction is a light-induced photoisomerization of the chromophore from 11-*cis* to all-*trans* conformation that triggers the Rh photocycle and structural changes of the protein enabling its interaction with the G-protein transducin.^{1,2} Chromophore photoisomerization in Rh is characterized by a high quantum yield of 0.65¹⁰ to be compared to that of 0.24 in methanol solution.¹¹

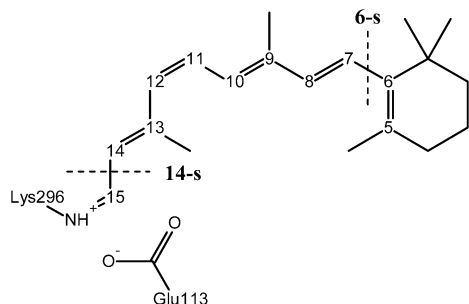
The observed red shift of absorption maximum from solution, 445 nm,¹¹ to protein Rh, 500 nm,⁹ the so-called opsin shift, is attributed to environmental effects on the chromophore. Recent gas-phase experiments on the absorption of retinal^{12,13} provide

[†] Lomonosov Moscow State University.

[‡] Russian Academy of Sciences.

- (1) Lewis, A. *Proc. Natl. Acad. Sci. U.S.A.* **1978**, *75*, 549.
- (2) Baylor, D. *Natl. Acad. Sci.* **1996**, *93*, 550.
- (3) Menon, N. T.; Han, M.; Sakmar, T. P. *Physiol. Rev.* **2001**, *81*, 1659.
- (4) Palczewski, K.; Kumasaka, T.; Hori, T.; Behnke, C. A.; Motoshima, H.; Fox, B. A.; Le Trong, I.; Teller, D.; Okada, T.; Stenkamp, R. E.; Yamamoto, M.; Miyano, M. *Science* **2000**, *289*, 739.
- (5) Teller, D. C.; Okada, T.; Behnke, C. A.; Palczewski, K.; Stenkamp, R. E. *Biochemistry* **2001**, *40*, 7761.
- (6) Okada, T.; Fujiyoshi, Y.; Silow, M.; Navarro, J.; Landau, E. M.; Schichida, Y. *Proc. Natl. Acad. Sci. U.S.A.* **2002**, *99*, 5982.
- (7) Okada, T.; Sugihara, M.; Bondar, A.-N.; Elstner, M.; Entel, P.; Buss, V. J. *Mol. Biol.* **2004**, *342*, 571.
- (8) Lin, S. W.; Sakmar, T. P.; Franke, R. R.; Khorana, H. G.; Mathies, R. A. *Biochemistry* **1992**, *31*, 5105.
- (9) Sakmar, T. P.; Franke, R. R.; Khonara, H. G. *Proc. Natl. Acad. Sci. U.S.A.* **1989**, *86*, 8309.
- (10) Kim, J. E.; Tauber, M. J.; Mathies, R. A. *Biochemistry* **2001**, *40*, 13774.
- (11) Freedman, K. A.; Becker, R. S. *J. Am. Chem. Soc.* **1986**, *108*, 1245.
- (12) Nielsen, I. B.; Lammich, L.; Andersen, L. H. *Phys. Rev. Lett.* **2006**, *96*, 018304.
- (13) Andersen, L. H.; Nielsen, I. B.; Kristensen, M. B.; El Ghazaly, M. O. A.; Haacke, S.; Nielsen, M. B.; Petersen, M. A. *J. Am. Chem. Soc.* **2005**, *127*, 12347.

Scheme 1. The Molecular Graph of the Rhodopsin Chromophore, Protonated Schiff Base of 11-*cis* Retinal, with Its Counterion, Glu113^a



^a The torsional angles along the C6–C7 and C14–C15 single bonds will be further referred to as 6-*s*- and 14-*s*-, respectively.

important information for theoretical studies of the influence of the protein environment on the chromophore properties as they serve to test the reliability of the calculations. The maximum of absorption band of the 11-*cis*-*N*-dimethyl retinal Schiff base in the gas-phase corresponds to the 610 nm¹² which is red-shifted with respect to that of the retinal in rhodopsin. One can distinguish several environmental contributions to absorption spectra of the retinal chromophore in various media, including the effect of the counterion, differences of the geometry configuration in condensed phase compared to the gas phase, and the effect of the electrostatic field caused by the environment.

Modeling the counterion effect on the retinal chromophore absorption spectra was described before in several papers.^{14–23} It has been found that the counterion strongly blue-shifts the gas-phase value of the vertical S0–S1 energy gap. This was explained by stabilization of the ground state and destabilization of the ionic state S1 associated with significant charge transfer from the Schiff base region through the polyene chain. Here we use the generally accepted characterization of the low-lying excited states of PSBR: the first excited-state in vacuo is similar to the ionic ¹B_u state of the linear polyene and the second excited-state is the covalent-like ²A_g-like state. This destabilization could lead to the switch of the S1 state character from ionic to covalent as it was proposed by Andruniow et al. for the model system of PSBR with the Glu113 counterion.¹⁸ It was also declared that the opsin shift is caused by the different influence of the protein and solution matrix on the counterion contributions, namely, the protein is supposed to counterbalance the counterion effect on the chromophore much stronger than the solvent particles.¹⁸

In modeling photoabsorption properties of retinal in solution and Rh, density functional theory (DFT)^{22–25} or DFT-based

MD,^{19–21} MP2,²⁶ and CASSCF^{16–18,23,26} methods have been applied for ground-state geometry optimization. Importantly, in these works the nearly planar PSBR conformation in solution is considered,^{18,26} while the spiral-like chromophore geometry configuration with overall negative helicity is admitted for Rh.^{16,25,27} In the latter conformations the main distortions from the planarity occur in the C10–C13 region (Scheme 1) leading to the formation of the salt bridge between the Schiff base NH and Glu113 counterion. However, we should note that the results of the X-ray studies^{4–7} do not provide unequivocal retinal conformation in the Rh binding site. The most discrepancies occur for the reported torsional angles around the C14–C15 (14-*s*) and C6–C7 (6-*s*) bonds. For example, in the PDBID: 1HZX structure⁵ the 14-*s* and 6-*s* angles (Scheme 1) are –99° and –30°, while in the PDBID:1F88 structure⁴ they are 180° and 77°, respectively. Therefore, we consider revisiting the impact of the ground-state equilibrium geometry configuration of retinal chromophore in the Rh binding site on the photoabsorption spectra as an important task.

We also note that the recent FTIR spectroscopy studies on the E181Q mutant of Rh reveal that a highly conserved residue Glu181 located in the vicinity of the chromophore group is likely to be negatively charged in the ground state and play an important role in the photoisomerization process being the counterion of PSBR in the MI photointermediate.²⁸ The deprotonated form of Glu181 was also suggested by MD simulation of Rh.²⁹ In all previous computational studies of retinal photoabsorption in Rh, except the work of Scheriber et al.,²² the uncharged Glu181 residue was assumed in geometry optimization.

In this work, besides reconsidering the role of the retinal chromophore structure in Rh, we employ highly accurate theoretical approaches to model absorption spectra of the retinal chromophore in the rhodopsin protein, in aqueous solution, and in the gas phase, attempting to provide a uniform computational level for all three model systems. As explained below, the estimates of excitation energies in quantum subsystems are performed here with an efficient version of the second-order multiconfigurational quasidegenerate perturbation theory³⁰ employing construction of effective Hamiltonians of large dimensions, the so-called augmented version of MCQDPT2 (aug-MCQDPT2). Environmental effects in the protein and solution are taken into account by using the mechanical embedding quantum mechanical–molecular mechanical (QM/MM)^{31–35} method and by using the effective fragment potential method.³⁶

Methods and Computational Details

To model the retinal chromophore properties inside rhodopsin, we considered the entire protein molecule with the initial coordinates of heavy atoms taken from subunit A of the crystallographic structure by

- (14) Cembran, A.; Bernardi, F.; Olivucci, M.; Garavelli, M. *Proc. Natl. Acad. Sci. U.S.A.* **2005**, *102*, 6255.
 (15) Cembran, A.; Bernardi, F.; Olivucci, M.; Garavelli, M. *J. Am. Chem. Soc.* **2004**, *126*, 16018.
 (16) Ferré, N.; Olivucci, M. *J. Am. Chem. Soc.* **2003**, *125*, 6868.
 (17) Coto, P. B.; Strambi, A.; Ferré, N.; Olivucci, M. *Proc. Natl. Acad. Sci. U.S.A.* **2006**, *103*, 17154.
 (18) Andruniow, T.; Ferré, N.; Olivucci, M. *Proc. Natl. Acad. Sci. U.S.A.* **2004**, *101*, 17908.
 (19) Hufen, J.; Sugihara, M.; Buss, V. *J. Phys. Chem. B* **2004**, *108*, 20419.
 (20) Sekharan, S.; Sugihara, M.; Buss, V. *Angew. Chem., Int. Ed.* **2007**, *46*, 269.
 (21) Sekharan, S.; Sugihara, M.; Weingart, O.; Okada, T.; Buss, V. *J. Am. Chem. Soc.* **2007**, *129*, 1052.
 (22) Schreiber, M.; Buss, V. *J. Chem. Phys.* **2003**, *119*, 12045.
 (23) Wanko, M.; Hoffmann, M.; Strodel, P.; Koslowski, A.; Thiel, W.; Neese, F.; Frauenheim, T.; Elstner, M. *J. Phys. Chem. B* **2005**, *109*, 3606.
 (24) Sugihara, M.; Buss, V.; Entel, P.; Elstner, M.; Frauenheim, T. *Biochemistry* **2002**, *41*, 15259.

- (25) Gascon, J. A.; Batista, V. S. *Biophys. J.* **2004**, *87*, 2931.
 (26) Losa, A. M.; Galván, I. F.; Martín, M. E.; Aguilar, M. A. *J. Phys. Chem. B* **2006**, *110*, 18064.
 (27) Sugihara, M.; Buss, V.; Entel, P.; Hafner, J.; Bondar, A. N.; Elstner, M.; Frauenheim, T. *Phase Transitions* **2004**, *77*, 31–45.
 (28) Lüdeke, S.; Beck, M.; Yan, E. C. Y.; Sakmar, T. P.; Siebert, F.; Vogel, R. *J. Mol. Biol.* **2005**, *353*, 345.
 (29) Röhrig, U. F.; Guidoni, L.; Rothlisberger, U. *Biochemistry* **2002**, *41*, 10799.
 (30) Nakano, H. *J. Chem. Phys.* **1993**, *99*, 7983.
 (31) Warshel, A.; Levitt, M. *J. Mol. Biol.* **1976**, *103*, 227.
 (32) Bakowies, D.; Thiel, W. *J. Phys. Chem.* **1996**, *100*, 10580.
 (33) Gao, J. L.; Xia, X. F. *Science* **1992**, *298*, 631.
 (34) Gao, J. *Acc. Chem. Res.* **1996**, *29*, 298.
 (35) Maseras, F.; Morokuma, K. *J. Comp. Chem.* **1995**, *16*, 1170.
 (36) Gordon, M. S.; Freitag, M. A.; Bandyopadhyay, P.; Jensen, J. H.; Kairys, V.; Stevens, W. *J. Phys. Chem. A* **2001**, *105*, 293.

Teller et al.⁵ (PDBID:1HZX). Positions of hydrogen atoms were preliminarily equilibrated by using the TINKER molecular modeling package (<http://dasher.wustl.edu/tinker/>). Beyond water molecules Wat2a and Wat2b registered by the X-ray crystallography,⁶ we added to the model system one more water molecule designated here as Wat2c. This step was motivated by examining available cavities in the retinal-binding pocket close to Wat2a. The quantum part for the QM/MM geometry optimization included the complete retinal chromophore, the side chains of Glu113, Glu181, and Ser186, and three water molecules (Wat2a, Wat2b, Wat2c). The interface between QM and MM subsystems was treated by the conventional link atom scheme.³²

The model system for retinal in aqueous solution included 11-*cis*-*N*-methyl protonated Schiff base of retinal and the counterion represented by the acetic acid. Those species were embedded into the cluster of 275 water molecules. The quantum part included PSBR, counterion, and the solvent molecule hydrogen-bonded to the Schiff base.

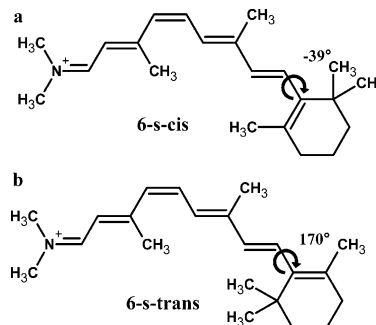
The equilibrium geometry parameters of the system modeling retinal in rhodopsin were optimized by using the QM/MM mechanical embedding approach³² with all nearby charged residues included into the quantum part. Since our aim was to obtain geometry configuration of the chromophore group inside the well-refined retinal-binding pocket most of the protein residues were fixed during optimization with the exception of side chains of Glu113, Glu181, Tyr192, Lys286, Ala292, and Phe293 located in the immediate proximity to the chromophore group.

Modeling the geometry configuration of PSBR in solution presents a more difficult problem because of unknown location of the counterion, high polarity of solvent molecules, and tremendous amount of local minima on the multidimensional potential-energy surface. We used molecular dynamics (MD) simulations by using TINKER program package and AMBER force field parameters³⁷ to equilibrate coordinates of solvent molecules in the absence of the counterion with the fixed coordinates of the chromophore. The MD computations were run for 12 ps at 300 K followed by gradual cooling to 0 K within 12 ps. Different starting positions of the counterion were considered with the counterion located at various distances from the Schiff base nitrogen atom. For such obtained model system, the geometry optimization was performed by using the effective fragment potentials approach.³⁶ In this technique, the wave function of the QM subsystem, selected here as PSBR, counterion, and one solvent molecule, are polarized by the MM environment (here, 274 water molecules) via the one-electron operators contributing to the QM Hamiltonian and representing the solute–solvent electrostatic, polarization, and exchange-repulsion interaction.

The gas-phase geometry configuration of the retinal chromophore was optimized for the 11-*cis*-*N*-dimethyl PSBR. For all model systems, the DFT method employing the PBE0 exchange–correlation functional³⁸ was used for quantum calculations including the gas-phase chromophore or the QM subsystems in QM/MM models. Correlation consistent cc-pVDZ basis sets with additional diffuse functions (aug-cc-pVDZ) on the oxygen atoms were employed.

The vertical excitation energies were computed at such obtained equilibrium geometry configurations of the ground electronic states. For all cases, including the gas-phase chromophore, the quantum parts of the protein and solution model systems, we used the aug-MCQDPT2 theory described in details elsewhere.³⁹ The first stage of this scheme presents the conventional CASSCF computation with the active space comprised by the full set of retinal π -orbitals for 12 π -electrons (the 12/12 approach). The electron density was averaged over two states in the case of retinal in the gas phase and over four states for retinal in solution and in the protein, since in the condense phases the correct ordering of the states was not attainable at the CASSCF level. The

Scheme 2. The 6-*s-cis* PSBR (a) and 6-*s-trans* PSBR (b) Structures of *N*-Dimethyl PSBR as Optimized for the Gas-Phase Conditions



MCQDPT2 calculations were carried out with such obtained CASSCF wavefunctions for the sequentially augmented effective Hamiltonians to obtain the stable solutions with regard to the number of reference states. The highest dimension of effective Hamiltonian was 15. The conventional intruder states avoidance⁴⁰ technique was used with the shift value of 0.02 au in the MCQDPT2 calculations.

Contributions to the excitation energies from the electrostatic field of the solvent and protein matrices were computed by using the effective fragment (EF) potential technique.³⁶ In the solvent case, we used the documented parameters of EFs representing the water molecules in the MM subsystem.³⁶ In the case of protein the procedure was more elaborated. In a series of preliminary ab initio calculations, the distributed multipoles representing each amino acid residue along the protein sequence as a separate effective fragment were calculated within the PBE0/cc-pVDZ approximation. The computed multipole expansions were then combined into single effective fragments representing the entire protein. Hybrid QM/MM and quantum chemistry computations for all model systems were performed with the PC GAMESS program package (A. A. Granovsky, URL <http://classic.chem.msu.su/gran/gamess/index.html>).

In the next section we present the results of simulations for the gas-phase (isolated chromophore) species, for the chromophore in aqueous solution, and for the rhodopsin protein. We discuss the calculated geometry configurations in the ground state and the vertical excitation energies for the S0–S1 transition. Among geometry-related quantities that affect the excitation energy we distinguish the 6-*s*-dihedral angle at the β -ionone ring (around the C6–C7 bond, Scheme 1) and the bond length alternation (BLA) parameter defined as a difference between the sum of the double bond lengths and single bond lengths for the conjugated chain excluding from the count the N=C double bond of Schiff base.

Results

The Isolated Chromophores. By using the PBE0/cc-pVDZ quantum chemistry approach for optimizing geometry parameters of the 11-*cis* protonated Schiff base retinal molecule we located two minimum-energy structures corresponding to the 6-*s-cis* and 6-*s-trans* conformations as illustrated in Scheme 2. The computed values of the 6-*s*-torsion angle were found as -39° and 170° , respectively. We verified that these stationary points on the potential-energy surface referred to the true minima with all real harmonic vibrational frequencies.

The ground-state energies of these two isomers differ by less than 1 kcal/mol (the 6-*s-cis* isomer being lower in energy) and, therefore, both of them may be observed in the gas phase. We should note that the 6-*s-trans* configuration with the 6-*s*-torsion angle 170° was previously reported by Wanko et al.²³ On the

(37) Wang, J.; Cieplak, P.; Kollman, P. A. *J. Comput. Chem.* **2000**, *21*, 1049.

(38) Adamo, C.; Barone, V. *J. Chem. Phys.* **1999**, *110*, 6158.

(39) Bochenkova, A. V.; Granovsky, A. A.; Bravaya, K. B.; Nemukhin, A. A. *J. Chem. Phys.* Submitted for publication.

(40) Witek, H. A.; Choe, Y.-K.; Finley, J. P.; Hirao, K. *J. Comp. Chem.* **2002**, *23*, 957.

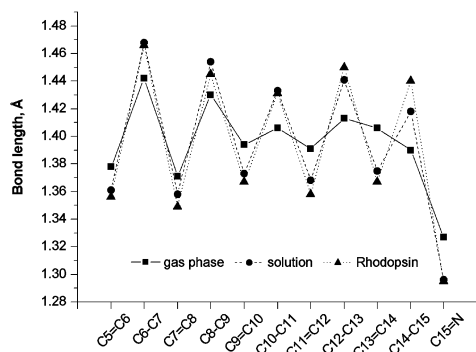


Figure 1. The computed bond lengths for retinal chromophore in gas phase (11-*cis*-6-*s-cis* PSBR), solution, and protein.

other hand, the only minimum energy structure for 11-*cis* PSBR reported by Cembran et al.⁴¹ following the CASSCF/6-31G* geometry optimization, corresponded to the 6-*s-cis* isomer with the 6-*s* torsion angle being equal to -68.7° . The value of the 6-*s* torsion angle was shown to strongly affect the vertical excitation energy of the gas-phase retinal chromophore,⁴¹ and up to 0.7 eV in excitation energy may be accounted for by variations of 6-*s*-torsion angle.

The bond lengths obtained in the PBE0/cc-pVDZ geometry optimization for the 11-*cis*-6-*s-cis* PSBR isomer are presented among other data in Figure 1. The strongly reduced BLA in the region C9–C15 is caused by the positive charge penetration through the conjugated π -system to the cyclohexene ring. The BLA of the gas-phase PSBR is estimated as 0.19 Å which is close to the value 0.26 Å for *n*-butyl-11-*cis* PSBR obtained by Sekharan et al.⁴² with the MP2 method. As discussed by Wanko et al.,²³ the hybrid exchange-correlation functionals (like one used in this work) should provide the BLA values very close to those computed in the CASPT2 approximation as well.

Table 1 contains the results of calculations for the S0–S1 excitation energy for the gas-phase retinal chromophore performed in this work and described in selected previous publications.

The theoretical results obtained here in the aug-MCQDPT2//PBE0/cc-pVDZ approximation for the 11-*cis*-6-*s-cis*-PSBR isomer (599 nm) provide a very good estimate of the absorption maximum in comparison to that observed experimentally for the gas-phase 11-*cis*-PSBR (610 nm).¹² It should be noted that the experimental gas-phase absorption spectra of PSBR show fairly complex structure in the region of higher energies,¹² in particular, due to contributions from vibrational states and possible occurrence of other isomers.

PSBR in Solution. To simulate retinal photoabsorption in the mixed water/methanol solution with acetic acid we consider the *N*-methyl-11-*cis*-PSBR moiety inside a cluster of water molecules (with and without additional species CH_3COO^- and CH_3OH). As deduced from energy minimization in the QM/MM approximation for all model systems analyzed in this work, the geometry configuration of the chromophore was found to be essentially planar with the enhanced bond length alteration (Figure 1) compared to the gas-phase species. An increase of BLA in condensed phases is usually attributed to the stabilization of the positive charge on the Schiff base NH group by the counterion^{19,22,24} or by the solvent molecules.²⁶

As mentioned in the preceding section, several choices for the QM subsystem were examined. Figure 2 illustrates the model system which we consider as the most advantageous for our purposes. The QM part includes PSBR, the counterion CH_3COO^- in the proximal position with respect to the chromophore, and the methanol molecule representing solvent species, which is hydrogen-bonded to the Schiff base NH group. There are 274 solvent water molecules described by the effective fragment potential (EFP) approach.³⁶ This model system is denoted here as {PSBR(s) + CH_3COO^- + CH_3OH }/EFP. Analysis of the computed equilibrium geometry configuration shows that the 6-*s* torsion angle -42° is close to that of the 6-*s-cis* isomers of the chromophore in the gas phase (-39°). We also note that the computed chromophore conformation is in agreement with the reported 6-*s-cis* configurations obtained by combined NMR studies and semiempirical calculations.⁴⁵

Another model system {PSBR(s) + CH_3COO^- + H_2O }/EFP also considered here differs from the previous one by occurrence of explicit water molecule in the QM part (instead of methanol) which is hydrogen-bonded to the Schiff base NH group. Correspondingly, the model system {PSBR(s)}/EFP refers to the case of PSBR trapped inside the shell of solvent water molecules (effective fragments) without the counterion. To emphasize an effect of the field of solvent molecules we also computed the S0–S1 excitation energies for the model systems PSBR(s) + CH_3COO^- + CH_3OH and PSBR(s) without any environment. The coordinates of these species were assumed as those corresponding to the equilibrium geometry configuration {PSBR(s) + CH_3COO^- + CH_3OH }/EFP. Table 2 collects the data for different model systems.

Comparison to the available experimental spectra of PSBR in methanol solution¹¹ shows that the effect of the field of solvent molecules as well as the presence of the counterion play a decisive role in the blue shift of the absorption maximum compared to the computed gas-phase value (610 nm). In addition to the results collected in Table 2 we verified a sensitivity of computed excitation energy to the position of the counterion CH_3COO^- in the model system. Depending on the distance from counterion to the Schiff base imine group the wavelengths of the S0–S1 excitation varied within the range 408–424 nm if the solvent molecule was excluded from the quantum part.

Rhodopsin. The results of QM(PBE0/cc-pVDZ)/MM(AMBER) geometry optimization for the chromophore and the nearest amino acid residues inside the rhodopsin cavity are well consistent with the available experimental data. According to the X-ray^{4–7} and the NMR studies^{46–50} of the Rh structures, the conformation of the retinal chromophore is highly distorted

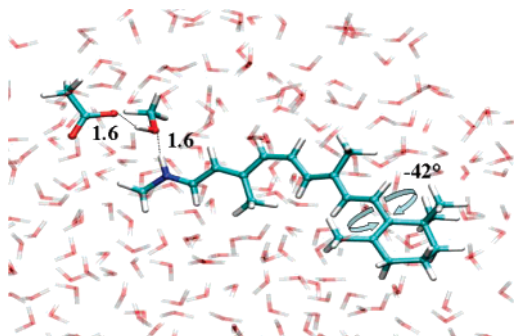
(41) Cembran, A.; González-Luque, R.; Altoe, P.; Merchan, M.; Bernardi, F.; Olivucci, M.; Garavelli, M. *J. Phys. Chem. A* **2005**, *109*, 6597.

(42) Sekharan, S.; Weingart, O.; Buss, V. *Biophys. J.* **2006**, *91*, L07.
 (43) Wanko, M.; Garavelli, M.; Bernardi, F.; Niehaus, T. A.; Frauenheim, T.; Elstner, M. *J. Chem. Phys.* **2004**, *120*, 1674.
 (44) Sun, M.; Ding, Y.; Cui, G.; Liu, Y. *J. Phys. Chem.* **2007**, *111*, 2946.
 (45) Honig, B.; Hudson, B.; Sykes, D.; Karplus, M. *Proc. Nat. Acad. Sci. U.S.A.* **1971**, *68*, 1289.
 (46) Creemers, A. F. L.; Kiihne, S.; Bovee-Geurts, P. H. M.; DeGrip, W. J.; Lugtenburg, J.; de Groot, H. J. M. *Proc. Natl. Acad. Sci. U.S.A.* **2002**, *99*, 9101.
 (47) Salgado, G. F. J.; Struts, A. V.; Tanaka, K.; Fujioka, N.; Nakanishi, K.; Brown, M. F. *Biochemistry* **2004**, *43*, 12819.
 (48) Spooner, P. J. R.; Sharples, J. M.; Verhoeven, M. A.; Lugtenburg, J.; Glaubitz, C.; Watts, A. *Biochemistry* **2002**, *41*, 7549.
 (49) Feng, X.; Verdegem, P. J. E.; Lee, Y. K.; Sandström, D.; Edén, M.; Bovee-Geurts, P.; de Grip, W. J.; Lugtenburg, J.; de Groot, H. J. M.; Levitt, M. H. *J. Am. Chem. Soc.* **1997**, *119*, 6853.
 (50) Feng, X.; Verdegem, P. J. E.; Edén, M.; Sandström, D.; Lee, Y. K.; Bovee-Geurts, P.; de Grip, W. J.; Lugtenburg, J.; de Groot, H. J. M.; Levitt, M. H. *J. Biomol. NMR* **2000**, *16*, 1.

Table 1. Comparison of the S0–S1 Excitation Energies ΔE and the Corresponding Wavelengths λ_{\max}^a

approach	system	ΔE , eV (λ_{\max} , nm)	reference
aug-MCQDPT2//PBE0/cc-pVDZ ^b	<i>N</i> -dimethyl-6- <i>s-trans</i> -11- <i>cis</i> -PSBR	2.22 (559)	this work
aug-MCQDPT2//PBE0/cc-pVDZ ^c	<i>N</i> -dimethyl-6- <i>s-cis</i> -11- <i>cis</i> -PSBR	2.07 (599)	this work
experiment	<i>N</i> -dimethyl-11- <i>cis</i> -PSBR	2.03 (610)	12
CASPT2//ANO//MP2/6-31G**	<i>N</i> -methyl-11- <i>cis</i> -PSBR	2.05 (606)	42
CASPT2//CASSCF/6-31G*	<i>N</i> -methyl-6- <i>s-cis</i> -11- <i>cis</i> -PSBR	2.28 (545)	41
CASPT2//DFT/6-31G*	6- <i>s-cis</i> -11- <i>cis</i> -PSBR	2.41 (515)	43
SORCI/SV(p)//CASSCF/6-31G*	6- <i>s-cis</i> -11- <i>cis</i> -PSBR	2.26 (549)	23
TDDFT/6-31+G**//DFT/6-31G*	6- <i>s-cis</i> -11- <i>cis</i> -PSBR	2.31 (537)	43
TDDFTB/6-31+G**//DFT/6-31G*	6- <i>s-cis</i> -11- <i>cis</i> -PSBR	2.05 (605)	43
TDDFT(SVWN)//DFT(B3LYP)/6-311++G*	<i>N</i> -dimethyl-6- <i>s-cis</i> -11- <i>cis</i> -PSBR	2.06 (603)	44

^a Calculations of the present work have been performed in the aug-MCQDPT2//PBE0/cc-pVDZ approximation. ^b The ground-state energy is -910.416297 au. ^c The ground-state energy is -910.416774 au.

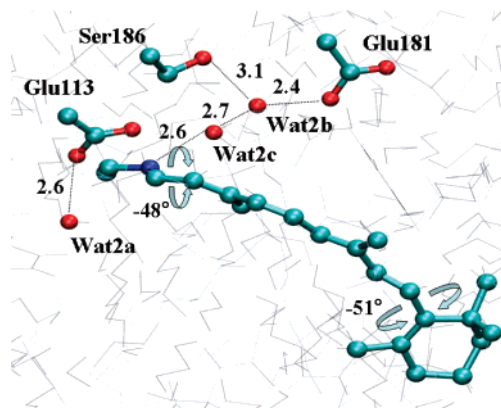
**Figure 2.** Equilibrium ground-state geometry configuration of retinal chromophore in the solution: the optimized model system {PSBR(s) + CH₃COO⁻ + CH₃OH}/EFP.**Table 2.** The S0–S1 Vertical Excitation Energies ΔE and the Corresponding Wavelengths for Different Model Systems Describing PSBR in Solution^a

model system and method	ΔE , eV (λ_{\max} , nm)	reference
PSBR(s)	2.13 (582)	this work
{PSBR(s)}/EFP	2.82 (440)	this work
PSBR(s) + CH ₃ COO ⁻ + CH ₃ OH	2.95 (421)	this work
{PSBR(s) + CH ₃ COO ⁻ + H ₂ O}/EFP	2.80 (444)	this work
{PSBR(s) + CH ₃ COO ⁻ + CH ₃ OH}/EFP	2.77 (448)	this work
experiments in methanol	2.79 (445)	11
<i>N</i> -methyl-11- <i>cis</i> -PSBR CASPT2//CASSCF/AMBER	2.89 (429)	18
11- <i>cis</i> -PSBR TDDFT//B3LYP/6-31G*/implicit solvent model	2.90 (428)	25

^a Calculations of the present work have been performed in the aug-MCQDPT2//PBE0/cc-pVDZ approximation.

from planarity. As shown in Figure 3, the PSBR moiety inside rhodopsin occurs in the 6-*s-cis* conformation near the β -ionone ring as suggested in experimental studies.^{4–7,46–48} The computed value of the 6-*s*-torsion angle is -51° . Arrangement of the β -ionone ring relative to the polyene chain is also in agreement with the results of rotational resonance solid-state NMR study.⁴⁸ The computed distances between the C8–C18 and C8–C17 atoms are 3.12 and 3.81 Å as compared to the experimental estimates 2.95 ± 0.15 and 4.05 ± 0.25 Å.⁴⁸ Calculation indicates significant nonplanarity of other conjugated fragments in the central part of the chromophore, in particular, in the region of the C9–C10 bond. Also, the computed H–C10–C11–H torsional angle, 166° , practically coincides with the value measured by the double-quantum heteronuclear local field NMR study, $160 \pm 10^\circ$.^{49,50}

We note a distortion from planarity in the region of the Schiff base of PSBR near the C14–C15 bond. The corresponding

**Figure 3.** Equilibrium ground state geometry configuration of the {PSBR(p) + Glu113 + Glu181 + Wat2a + Wat2b + Wat2c}/MM model system.

torsional angle (14-*s*-), -48° , qualitatively agrees with that of the PDBID:1HZX model of the retinal chromophore (-99°). In our model, this feature is explained by the hydrogen bonding of PSBR to the water molecule Wat2c (Figure 3), which is a part of the hydrogen-bond network connecting PSBR to the Glu181 residue. Indeed, a site-directed mutagenesis study⁵¹ revealed that mutations of Tyr192 and Tyr268 residues coordinating the Glu181 carboxyl group resulted in reduction of activation of transducin by Rh. Following these observations, it was concluded that Glu181 should be an important member of the hydrogen-bond network in the Rh cavity.⁵¹ As expected, PSBR in Rh is characterized by an enhanced BLA of 0.435 Å as compared to the gas-phase species (Figure 1) owing to stabilization of the positive charge at the NH Schiff base moiety.

Table 3 contains the calculation results in the aug-MC-QDPT2//PBE0/cc-pVDZ approximation for the S0–S1 vertical excitation energies ΔE and corresponding wavelengths λ_{\max} for different model systems. In all cases the geometry configuration of PSBR obtained in the QM(PBE0/cc-pVDZ)/MM(AMBER) energy optimization in the protein was used, PSBR(p). As shown in Table 3, introducing the counterion Glu113 and the nearest two water molecules to the model system (PSBR(p) + Glu113 + Wat2a + Wat2c) results in the strong blue shift of about 200 nm. Although being very important for the equilibrium geometry configuration of PSBR in the ground state, the charged residue Glu181 was not found to be essential for calculations of the excitation energy (compare the second and third rows of Table 3). This result is in complete agreement with the UV spectra of E181N Rh mutant with the absorption maximum 508

(51) Janz, J. M.; Farrens, D. L. *J. Biomol. Chem.* **2004**, *279*, 55886.

Table 3. The S0–S1 Vertical Excitation Energies ΔE and Corresponding Wavelengths λ_{\max} for Different Model Systems^a

model system	ΔE , eV (λ_{\max} , nm)	reference
PSBR(p)	2.01 (616)	this work
PSBR(p) + Glu113 + Wat2a + Wat2c	3.07 (404)	this work
PSBR(p) + Glu113 + Glu181 + Wat2a + Wat2b + Wat2c	3.19 (388)	this work
{PSBR(p) + Glu113 + Glu181 + Wat2a + Wat2b + Wat2c}/MM	2.41 (515)	this work
experiment	2.45 (500)	9
CASPT2/ANO// SCC-DFTB/CHARMM	2.47 (502)	20, 21
CASPT2/CASSCF/6-31G*/AMBER	2.59 (479)	18
TDDFT//B3LYP/6-31G*/AMBER	2.58 (481)	53
SAC-CI//B3LYP(D95(d))/AMBER	2.45 (500)	54

^a Calculations in this work have been performed in the aug-MCQDPT2//PBE0/cc-pVDZ/AMBER approximation. The notation PSBR(p) means that the geometry configuration of PSBR was obtained in the QM(PBE0/cc-pVDZ)/MM(AMBER) geometry optimization in the protein matrix.

nm being only slightly shifted from the wild-type Rh.⁵² On the other hand, the protein field acts in the opposite direction compared to the counterion leading to the red shift as seen in the third and fourth rows of Table 3.

Discussion and Conclusions

As described in the preceding section we report the results of accurate calculations of the excitation energies for the S0–S1 transitions of the 11-*cis* retinal in the gas phase, in solution, and in rhodopsin performed at a uniform computational level, aug-MCQDPT2//PBE0/cc-pVDZ, for all three model systems. The computed positions of λ_{\max} obtained at the highest level of the theory, 599(g), 448(s), and 515(p) nm for the gas phase, solution, and protein, respectively, are in excellent agreement with the corresponding experimental data, 610(g), 445(s), and 500(p) nm. Such consistency provides a support for qualitative conclusions that can be drawn by the results of these simulations.

The mechanism of spectral tuning of retinal either by protein, or solvent molecules^{16–18,20,21,23,25,26,54,55} as well as chromophore conformations and chromophore–protein interactions,^{18,20–23,27,58} have been modeled before by using various QM/MM approaches. In particular, the CASPT2^{16–18,20,21,23,26,55} or time-dependent density functional theory (TDDFT)²⁵ methods have been used for calculation of excitation spectra. Accurate estimates of absorption maxima were achieved by using the CASPT2 multiconfigurational perturbation theory for the CASSCF/6-31G* optimized ground-state geometry for retinal in rhodopsin (479, 502 nm)^{17,18,20,21} and solution (429, 434 nm).^{18,42} In the present study we revisited the possible geometry configuration of retinal chromophore in different environment and used a high level quantum chemistry method (aug-MCQDPT2) to examine an influence of different factors on the vertical excitation energies of PSBR.

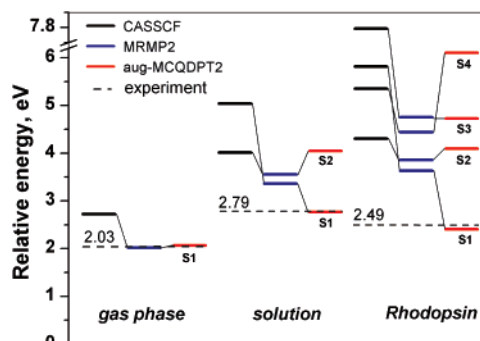


Figure 4. The energies of the low-lying excited states obtained in the CASSCF, MRMP2, and aug-MCQDPT2 approximations (in all cases with the cc-pVDZ basis set augmented by diffuse functions on oxygen atoms) relative to the corresponding ground-state energies. Black bars refer to the CASSCF results, blue bars to the MRMP2 estimates, and red bars to the aug-MCQDPT2 data. The dashed lines specify the experimental values.

A better accuracy of the aug-MCQDPT2 approach compared to the state-specific multiconfigurational perturbation theory MRMP2⁵⁹ is illustrated in Figure 4. It is known that the state-averaging CASSCF procedure may result in the wrong ordering of the excited states as exemplified here for the chromophore in solution and in the protein. The use of the MRMP2 approach may be insufficient to correct these deficiencies. On the contrary, the effective Hamiltonian technique implemented in the aug-MCQDPT2 approach can account for qualitative change in the electronic-state wave function by state mixing and provides quantitative correct excitation energies. The data presented in Figure 4 also illustrate different impacts of perturbation theory corrections on the first and second excited states (as finally obtained in the aug-MCQDPT2 calculations). The first excited state is known to possess ionic character and can be described as the $1B_u$ -like moiety by analogy to the linear polyenes, whereas the ground and the second excited state possess covalent character ($2A_g$ -like) for the gas-phase chromophore. It was shown before that ionic B_u states were more sensitive to the dynamic electron correlation⁶⁰ than the A_g states. As seen in Figure 4, the A_g – B_u electron transitions are shifted by approximately 1.8 and 2.2 eV for solution and Rh model systems, respectively, even in the MRMP2 calculations, while the A_g – A_g transition energies decreased by only 0.5 and 0.4 eV. In the aug-MCQDPT2 approximation, the first excited-state possesses the B_u -like ionic character in all model systems considered in this work. This is valid even for the model system with the largest S0–S1 energy gap, namely, PSBR(p) + Glu113 + Glu181 + Wat2a + Wat2b + Wat2c (Table 3). The latter observation contrasts to the CASPT2 results¹⁸ for the model system of the PSBR chromophore with the Cl^- counterion, for which the lowest excited-state is considered to be the A_g -like state. According to our results, spectral tuning of the retinal chromophore is guided by the environmental effects on the $1B_u$ state.

Despite of fairly large amount of papers devoted to computational studies on rhodopsin the reasons of the opsin shift are still under discussion. One of the hypothesis based on computational studies by the CASPT2//CASSCF/6-31G*/AMBER method is that the chromophore experiences a stronger counterbalancing of the counterion influence by the protein environ-

- (52) Yan, E. C. Y.; Kazmi, M. A.; De, S.; Chang, B. S. W.; Seibert, C.; Marin, E. P.; Mathies, R. A.; Sakmar, T. P. *Biochemistry* **2002**, *41*, 3620.
 (53) Gascón, J. A.; Sproviero, E. M.; Batista, V. S. *Acc. Chem. Res.* **2006**, *39*, 184.
 (54) Fujimoto, K.; Hayashi, S.; Hasegawa, J.; Nakatsuji, H. *J. Chem. Theor. Comput.* **2007**, *3*, 605.
 (55) Sugihara, M.; Hufen, J.; Buss, V. *Biochemistry* **2006**, *45*, 801.
 (56) Saam, J.; Tajkhorshid, E.; Hayashi, S.; Schulten, K. *Biophys. J.* **2002**, *83*, 3097.
 (57) Yamada, A.; Kakitani, T.; Yamamoto, S.; Yamato, T. *Chem. Phys. Lett.* **2002**, *366*, 670.
 (58) Buss, V.; Sugihara, M.; Entel, P.; Hafer, J. *Angew. Chem., Int. Ed.* **2003**, *42*, 3245.

- (59) Finley, J. P.; Hirao, K. *Chem. Phys. Lett.* **2000**, *328*, 51.
 (60) Nakayama, K.; Hirao, H.; Hirao, K. *Int. J. Quant. Chem.* **1998**, *66*, 157.
 (61) Menon, S. T.; Han, M.; Sakmar, T. P. *Physiol. Rev.* **2001**, *81*, 1659.

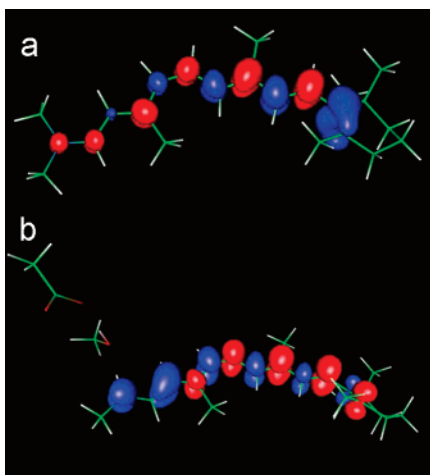


Figure 5. Difference of the π -type electron densities for the first S1 and S0 excited states computed in the aug-MCQDPT2 approximation: (a) gas-phase 11-*cis*-6-*s-cis* PSBR; (b) PSBR model system in solution {PSBR(s) + CH₃COO⁻ + CH₃OH}/EFP. Red color corresponds to an increase of the electron density in the S0–S1 electron transition; blue color indicates a decrease of the density.

ment than that by solvent molecules, and therefore this explains the blue shift of the absorption maximum from Rh to solution.¹⁸ However, we cannot confirm such strong counterbalancing or shielding of the counterion by the protein, in which the counterion is located at ~ 3.5 Å from the Schiff base. Moreover, the effective shielding is likely to occur in solution, where the distance between the counterion and the Schiff base is larger and the ions seem to be well separated by solvent molecules. Indeed, the complete shielding of the counterion by solvent molecules is observed in the present study.

When considering the opsin shift, one may distinguish the following factors: the change of the chromophore geometry conformation, environmental electrostatic field, and the counterion effects. In our work, the chromophore geometry distortions for PSBR in solution and in protein compared to the gas phase were found to produce the minor shift of the absorption maximum on the overall scale of the spectral shift. This is illustrated by a comparison of the calculated S0–S1 excitation wavelengths for the PSBR(s) (582 nm) and PSBR(p) (616 nm) model systems with that of the gas-phase chromophore (599 nm): the change of the geometry conformation accounts for the blue and red absorption shift of less than 20 nm for solution and Rh respectively.

It is established that the counterion strongly blue shifts the S0–S1 excitation energy.^{14–23} According to the previous results¹⁸ the S0–S1 energy gap increase is due to the stabilization of the S0 and S2 Ag-like states in which the positive charge is located at the N=C Schiff base. Our results are in agreement with the enhancement of the S0–S1 energy gap. However, as seen in Figure 5, the origin of this spectral shift is not limited to the S0 stabilization, but also includes evolution of the first excited state. According to our results, the S1 state for retinal in solution is characterized by the electron-density transfer not to the Schiff base region as occurs in the gas-phase chromophore, but to the β -ionone ring, probably due to the repulsion interaction of electron density with the counterion. It can be concluded that the presence of the counterion changes the character of the first excited state to the different 1Bu-like state.

The absorption shift from the gas phase to solution can be

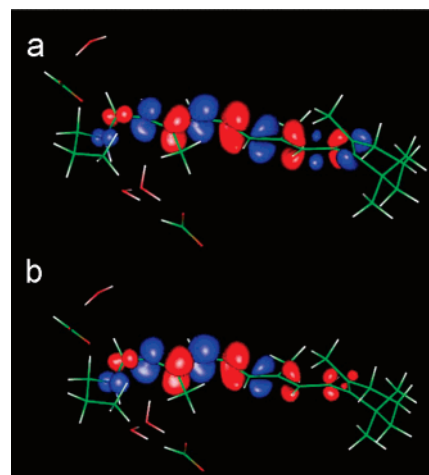


Figure 6. Difference of the π -type electron densities for the first S1 and S0 excited states computed in the aug-MCQDPT2 approximation for PSBR model systems inside the Rh cavity: (a) PSBR(p) + Glu113 + Glu181 + Wat2a + Wat2b + Wat2c; (b) PSBR in the {PSBR(p) + Glu113 + Glu181 + Wat2a + Wat2b + Wat2c}/MM model system. Red color corresponds to an increase of the electron density in the S0–S1 electron transition; blue color indicates a decrease of the density.

almost entirely attributed to the solvent impact on the chromophore spectral properties, what is indicated by comparison of the vertical excitation energies of the model systems {PSBR}/EFP, PSBR(s) + CH₃COO⁻ + CH₃OH and {PSBR(s) + CH₃COO⁻ + CH₃OH}/EFP (Table 2). In other words, solvent acts in line with the counterion by stabilizing the ground state with the Ag-like character.

In the protein case, counterions provide a strong blue shift of approximately 200 nm found for the PSBR(p) + Glu113 + Glu181 + Wat2a + Wat2b + Wat2c model system (Table 3). The impact of the protein environment in the model system through the MM(EFP) approach leads to the strong backward red shift of the absorption maximum unlike that in recent findings by Sekharan et al.^{20,21} Therefore in line with recent QM/MM studies of Rh photoabsorption^{16,17} the protein environment diminishes the counterion effects on the chromophore group.

The overall features of the S0–S1 electronic transition of the chromophore in the protein differ from those of the gas-phase chromophore and from the chromophore in solution: most of electron density redistribution occurs in the C11–C12–C13 region (Figure 6). There are two possible explanations of this observation. First, the nonplanarity of the C14–C15 single bond that can strongly alter the electronic density redistribution by reducing the conjugation along the polyene chain. Second, this is due to an influence of the negatively charged residue Glu181 located close to the chromophore group. From this point of view, the decrease of the excitation energy would be gained if the protein matrix assists electronic density redistribution. Indeed, inclusion of the protein field to the model leads to an increase of the density redistribution in the C11–C12 region (Figure 6). This result is in variance with the strong positive charge delocalization along the polyene chain to the β -ionone ring upon excitation of the Rh chromophore as reported by Coto et al.¹⁷ However, the model with the uncharged (protonated) state of Glu181 was used in the latter study¹⁷ in what could significantly alter the results. Another possible reason of the red shift in the absorption maximum caused by protein is a recovery of partially

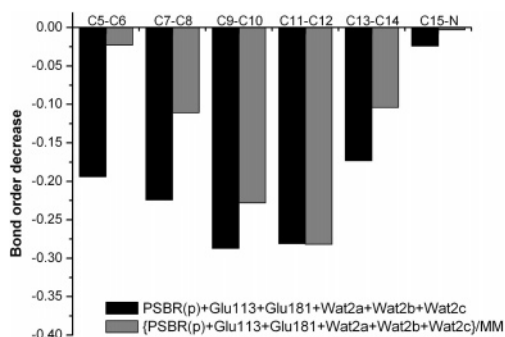


Figure 7. Decrease of the double-bond orders upon S0–S1 excitation of retinal chromophore inside the Rh cavity computed with the aug-MCQDPT2 natural orbitals.

disrupted π -conjugation in the Schiff-base chromophore region (nonplanar C14–C15 single bond) in the ground electronic state. Indeed, the bond orders of C15–N and C14–C15 in PSBR(p) + Glu113 + Glu181 + Wat2a + Wat2b + Wat2c are 1.64 and 1.14, respectively, as compared to the 1.58 and 1.20 computed for the same model system with the protein electrostatic field taken into account ({PSBR(p) + Glu113 + Glu181 + Wat2a + Wat2b + Wat2c}/MM). Therefore the nonplanarity in the Schiff-base region along with the preorganized protein matrix can account for the red shift of the absorption maximum as seen from comparison of S0–S1 excitation energies for the full model protein system {PSBR(p) + Glu113 + Glu181 + Wat2a + Wat2b + Wat2c}/MM and the reduced model system PSBR(p) + Glu113 + Glu181 + Wat2a + Wat2b + Wat2c.

Consideration of the electrostatic field of the protein matrix also results in certain localization of the bond-order changes upon excitation. The decrease of double-bond orders computed for Rh model systems with and without protein field is shown

in Figure 7. As one can see, the effect of protein is to compress the region with the significantly decreased bond orders and to locate the maximum at the C11–C12 double bond. The latter can be one of the reasons of the C11–C12 photoisomerization specificity. The stronger electronic density redistribution in the case of the model system {PSBR(p) + Glu113 + Glu181 + Wat2a + Wat2b + Wat2c}/MM is proven by a higher value of transition dipole moment: 3.43 D compared to 2.98 D for the PSBR(p) + Glu113 + Glu181 + Wat2a + Wat2b + Wat2c model system. Therefore, we conclude that the protein environment acts in favor of the ionic 1Bu-like electron transition with the main electron density redistribution within the region of the C11–C12 double bond, finally leading to a decrease of the excitation energy.

We emphasize that accurate calculations of the positions of the S0–S1 absorption band λ_{\max} for the considered model systems provide a firm base for qualitative conclusions on the features of this important biological chromophore in different media.

Acknowledgment. The substantial contributions of J. Kress to the QM/MM extended PC GAMESS version are greatly acknowledged. A.B. and A.N. thank Professor M. Olivucci for valuable discussions. A.B. and K.B. acknowledge financial support from the Russian Science Support Foundation. This study was partially supported by the Grant 05-03-39010 from the Russian Foundation for Basic Research.

Supporting Information Available: Cartesian coordinates of geometries of 11-*cis* retinal in the gas phase, solution, and protein. This material is available free of charge via the Internet at <http://pubs.acs.org>.

JA0732126